



Spatial and seasonal variations of PM_{2.5} mass and species during 2010 in Xi'an, China



Ping Wang^a, Jun-ji Cao^{a,c,*}, Zhen-xing Shen^d, Yong-ming Han^b, Shun-cheng Lee^e, Yu Huang^e, Chong-shu Zhu^a, Qi-yuan Wang^a, Hong-mei Xu^d, Ru-jin Huang^{f,g}

^a Key Lab of Aerosol Science & Technology, Institute of Earth Environment, Chinese Academy of Sciences, Xi'an, China

^b State Key Lab of Loess and Quaternary Geology, Institute of Earth Environment, Chinese Academy of Sciences, Xi'an, China

^c Institute of Global Environmental Change, Xi'an Jiaotong University, Xi'an, China

^d Department of Environmental Science and Engineering, Xi'an Jiaotong University, Xi'an, China

^e Department of Civil and Environmental Engineering, The Hong Kong Polytechnic University, Hong Kong

^f Lab of Atmospheric Chemistry, Paul Scherrer Institute (PSI) Villigen, 5232 Villigen, Switzerland

^g Centre for Climate and Air Pollution Studies, Ryan Institute, National University of Ireland Galway, University Road, Galway, Ireland

HIGHLIGHTS

- Spatial variations in PM_{2.5} mass concentrations were not obvious, but PM_{2.5} mass and chemical species showed a similar seasonal pattern at all six sites, decreasing from winter > autumn > spring > summer.
- The dominant PM_{2.5} components were organic carbon in winter, soil dust in spring, and sulfate, nitrate and ammonium in summer and autumn.
- Emissions from fossil fuel burning are the most important source for PM_{2.5}.
- A decreasing trend in OC/PM_{2.5} is observed compared with previous studies in Xi'an.

ARTICLE INFO

Article history:

Received 8 March 2014

Received in revised form 1 November 2014

Accepted 2 November 2014

Available online 13 December 2014

Editor: Xuexi Tie

Keywords:

Xi'an

PM_{2.5}

Air pollution

PMF

ABSTRACT

PM_{2.5} mass and selected chemical species are measured in 24-h integrated PM_{2.5} samples collected simultaneously at the urban and rural regions of Xi'an (six sites in total), China in the four seasons of 2010. The analytes include organic carbon and elemental carbon (OC + EC = total carbon, TC), seven water-soluble inorganic ions (NH₄⁺, K⁺, Mg²⁺, Ca²⁺, Cl⁻, SO₄²⁻, NO₃⁻) and six trace elements (Ti, Mn, Fe, Zn, As, Pb). The average PM_{2.5} mass for the entire measurement period is 142.6 ± 102.7 μg m⁻³, which is more than four times that of the Chinese national ambient air quality standard. Spatial variations in PM_{2.5} mass are not pronounced. The PM_{2.5} mass and those species measured show a similar seasonal pattern in all six measurement sites, i.e., in the order of winter > autumn > spring > summer. The dominant PM_{2.5} composition is OC in winter, soil dust in spring, and sulfate, nitrate, and ammonium in summer and autumn. Seasonal variations of TC/PM_{2.5} and OC/EC ratios follow the PM_{2.5} changes. Seasonal distributions of (SO₄²⁻ + NO₃⁻ + NH₄⁺)/PM_{2.5} showed increase in autumn and decrease in winter, while NO₃⁻/SO₄²⁻ ratios increased in autumn and decreased in summer. Eight main PM_{2.5} sources are identified based on the positive matrix factorization (PMF) analysis and emissions from fossil fuel combustion (traffic and coal burning) are founded to be the main source responsible for the fine particle pollution in Xi'an. In addition, a decreasing trend in OC/PM_{2.5} is observed in comparison with previous studies in Xi'an.

© 2014 Elsevier B.V. All rights reserved.

1. Introduction

Atmospheric PM_{2.5} (particulate matter with aerodynamic equivalent diameters ≤ 2.5 μm) is an important determinant of air quality because these particles can affect human health, climate, and visibility; their

effects are functions of the concentrations, composition, sizes, and shapes of the particles. Satellite observations have shown that the Guanzhong Plain in central China is one of the most severely polluted regions in the world, having an annual average PM_{2.5} mass concentration of > 80 μg m⁻³ (Van Donkelaar et al., 2010). Spatial and temporal variations of PM_{2.5} mass and species composition have been the main focus of efforts to understand the environmental effects of air pollution. In China, studies of PM_{2.5} have been carried out since 2000, and they have mainly focused on economically-developed urban clusters. These studies have involved (a) PM_{2.5} carbonaceous components (Cao et al.,

* Corresponding author at: Key Lab of Aerosol Science & Technology, Institute of Earth Environment, Chinese Academy of Sciences, Xi'an, China. Tel.: +86 29 8832 6488; fax: +86 29 8832 0456.

E-mail address: cao@loess.llqg.ac.cn (J. Cao).

2003, 2004; Duan et al., 2007; Ho et al., 2011), water-soluble inorganic ions (Hu et al., 2008; Liu et al., 2008) and trace elements (Ho et al., 2003; Wong et al., 2003) in the Pearl River Delta; (b) PM_{2.5} physical and chemical properties (Chan and Yao, 2008; Yao et al., 2002), precursors of model estimations (Tie et al., 2013), source apportionments based on stable carbon isotopes (Cao et al., 2013), and dust-pollutant mixtures (Huang et al., 2010; Wang et al., 2005) in the Yangtze River Delta; and (c) PM_{2.5} chemical composition (Duan et al., 2006; He et al., 2001; Yang et al., 2011a), source identification (Zhang et al., 2013; Zheng et al., 2005), haze episodes (Li et al., 2011; Sun et al., 2006; Dong et al., 2013) and dust storms (Sun et al., 2000; Zhang et al., 2005) in the areas around Beijing, Tianjin, and Hebei. Although these studies have provided useful information for specific cities, data for different types of sites (urban, rural and reference) as well as seasonally representative data and full chemical characterizations of PM_{2.5} are still limited.

Xi'an (34°16' N, 108°54' E, 396.9 m a.s.l.), is a megacity located in the Guanzhong Plain; it has a temperate, semiarid climate, and the prevailing winds are northeasterly. The city is surrounded by the Qinling Mountains to the south, and the Loess Plateau extends to the north and west; these topographical features limit the dispersal of air pollutants, and as a result pollutants can become trapped, leading to serious health concerns. A number of studies have been carried out to understand the physicochemical properties of PM_{2.5} and the triggers for pollution episodes over Xi'an (Cao et al., 2005b, 2012b).

For example, Cao et al. (2005b) found that the high organic carbon to elemental carbon (OC/EC) ratios occurred in winter due to the large quantities of fossil fuels and biofuels burned for domestic heating. Shen et al. (2011) investigated the chemical composition of PM₁₀ and PM_{2.5} collected at ground level and at 100 m during a strong wintertime pollution episode, and these authors concluded that the air quality in Xi'an could be improved by reducing the emissions from coal and biomass burning. Han et al. (2006) investigated trace element signatures of urban dusts during May of 1998, 1999 and 2001, and they showed elevated concentrations as a whole, with arsenic and manganese as notable exceptions. Kawamura et al. (2012) measured the molecular distributions and stable carbon isotopic composition of water-soluble organic aerosols in size-resolved airborne particles (9-stages) during summer and winter. Xu et al. (2012) assessed the PM_{2.5} lead concentrations after the phasing out of leaded gasoline, and their results showed that coal combustion has become the major Pb source in winter while vehicular emissions remained the major Pb source in summer. Huang et al. (2012) conducted a time-series analysis to examine the seasonal variations in the mortality risks associated with PM_{2.5} and the loadings of specific chemical species. In short, the previous studies in Xi'an have generally focused on a single sampling site, and the synchronous measurements at multiple sites we report here are a major step towards a more comprehensive understanding of PM_{2.5} pollution in the city.

The findings in this paper complement prior results by adding information on the spatial and seasonal variability of PM_{2.5} over Xi'an; the results include measurements of carbonaceous, ionic, and elemental components extracted from quartz filters that are simultaneously collected at six sampling sites. The objectives of this study are to (1) characterize spatial and seasonal variations in the concentrations of PM_{2.5} and a suite of chemical substances, (2) identify the likely sources for the PM_{2.5} aerosol and apportion their respective contributions, and (3) compare the results with those from other studies to broaden our understanding of PM_{2.5} pollution. The knowledge gained from this study also provides information that the government can use to develop pollution control measures and possibly emergency response plans.

2. Material and methodology

2.1. The monitoring locations and PM_{2.5} sampling

The locations of the urban and rural sampling sites are shown in Fig. 1; these sites are selected based on their topography, meteorology,

population, energy use, industries, mix of vehicles, and vehicular density. The environmental characteristics of the six sampling sites are presented in Table 1; they can be separated into three categories: (1) an upwind site in Gaoling county (GLC) to the northeast of the Xi'an, (2) a reference station at the Black River Reservoir (BRR) to the southwest, and (3) four urban sites, namely the Institute of Earth Environment, the Chinese Academy of Science (IEE) to the south of the city center, Micro Motor factory (MMF) to the west, the Municipal Government Hall (MGH) in the downtown area, and the Chan-ba ecological district (CBE) to the east. The strategy behind the sampling at the GLC station is that it is upwind of the major local sources for pollutants under the prevailing airflow, and therefore it can be considered representative of the inflow to the region. The BRR station is selected as a reference station: it is located on the edge of Qingling Mountains, 100 km from the center of the city, but it is downwind of Xi'an and therefore likely affected to a degree by anthropogenic activities and emissions in the city. This is why we refer to it as a reference station rather than a background station.

Daily PM_{2.5} samples are taken for two weeks during each of four months in 2010 as follows (1) 12 to 25 January; (2) 14 to 27 April; (3) 12 to 25 July; and (4) 12 to 25 October, 2010; these months are assumed to be representative of winter, summer, spring and fall, respectively. Four mini-volume samplers (Airmetrics, Oregon, USA) operating at flow rates of 5 L min⁻¹ are located ~10 m above ground level at the urban sampling sites. At the rural sites, two Tisch (TE-6001, Tisch Environmental, Inc., USA) high-volume PM_{2.5} samplers (1000 L min⁻¹) are deployed. Filter blanks are collected in each season from each site. PM_{2.5} samples are collected on pre-fired, pre and post-weighed Whatman™ quartz-fiber filters for 24 h from 10:00 am to 10:00 am (local time) every day. A total of 342 PM_{2.5} filters (including 6 blanks) are collected at the six sampling sites.

2.2. Chemical analysis and quality control

The mass concentrations of the sample filters are determined gravimetrically with the use of an electronic microbalance with 1 µg sensitivity (MC5; Sartorius, Goettingen, Germany) under controlled temperature (20–23 °C) and relative humidity (RH at 35–45%). Three anions (Cl⁻, NO₃⁻ and SO₄²⁻) and four cations (NH₄⁺, K⁺, Mg²⁺ and Ca²⁺) are determined by ion chromatography (DX-600 Ion Chromatograph, Dionex Inc., Sunnyvale, CA, USA). Organic carbon (OC) and elemental carbon (EC) are analyzed using the IMPROVE_A thermal optical reflectance (TOR) method (Cao et al., 2007), and total carbon (TC) is calculated as the sum of OC plus EC. Energy Dispersive X-Ray Fluorescence (ED-XRF) spectrometry (Epsilon 5 ED-XRF, PANalytical B. V., the Netherlands) is used to determine the concentrations of selected trace elements. Filter blanks are also analyzed for each season, and the sample data are corrected from these blanks. All these measurements are conducted at the Institute of Earth Environment, Chinese Academy of Sciences.

Quartz-fiber filters contain high backgrounds of Al, Ca, Mg, and Na, but our analyses showed that the sample-to-blank ratios for the other trace elements (Ti, Mn, Fe, Zn, As, and Pb) are larger than 3, making the results usable. More detailed information on the various measurements, as well as quality assurance and quality control procedures can be found in Zhang et al. (2011) for ion analyses, Xu et al. (2012) for the elemental analyses, and Cao et al. (2009) for carbon analyses.

2.3. Source apportionment

Positive matrix factorization (PMF), a statistical technique developed by Paatero and colleagues (Paatero and Tapper, 1994), is a widely used source-apportionment receptor model that does not require information on the source profiles prior to analysis and has no limitation relative to the number of sources (Hopke, 2003; Shen et al., 2011). PMF has been widely used to identify presumptive sources for various aerosol constituents (Hwang and Hopke, 2007; Antony Chen et al., 2007,

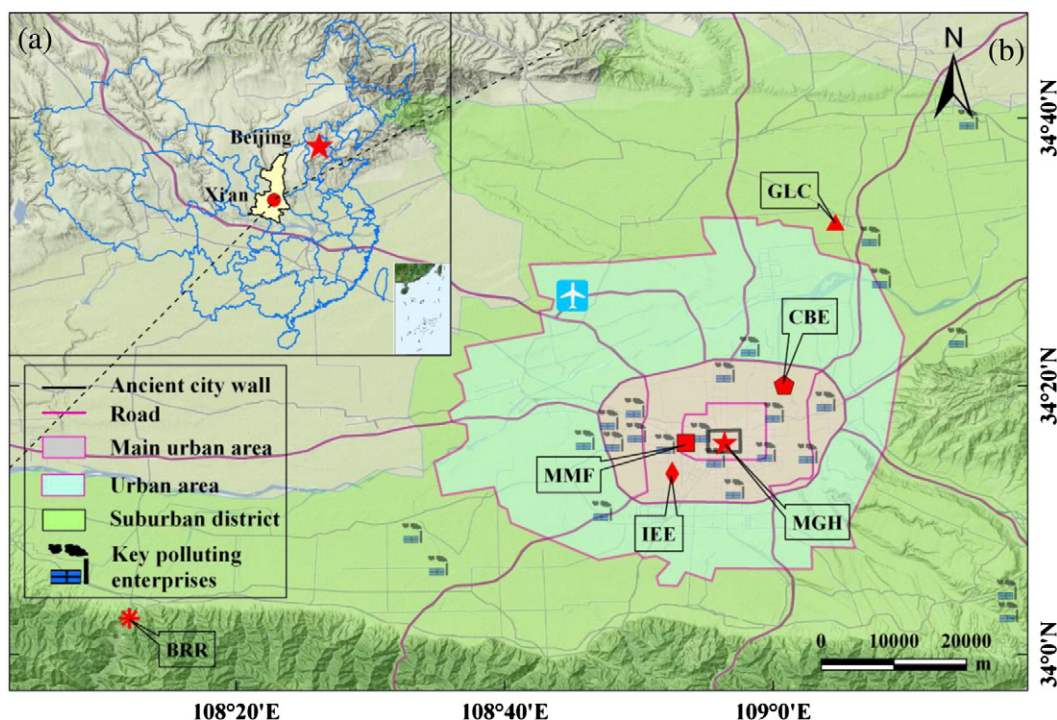


Fig. 1. Map (a) showing location of Xi'an, China and (b) six sampling locations in and near Xi'an. Two rural sampling sites: upwind station in Gaoling county (GLC) (34°32'05.34" N, 109°05'12.11" E), reference station at Black River reservoir (BRR) (34°02'51.05" N, 108°12'21.27" E); four urban sampling sites: Chan-ba ecological district (CBE) (34°20'18.54" N, 109°01'21.66" E), municipal government hall (MGH) (34°16'01.08" N, 108°56'58.49" E), micro motor factory (MMF) (34°15'59.65" N, 108°53'55.22" E), Institute of Earth Environment, Chinese Academy of Sciences (IEE) (34°13'49.77" N, 108°52'58.72" E).

2010). The principles of the PMF model have been discussed in detail elsewhere (Cao et al., 2012b; Shen et al., 2010). Here, PMF version 3.0 is employed, and the concentrations of 15 chemical species are the input to the model; the analytes included in the analyses are: OC, EC, Cl^- , SO_4^{2-} , NO_3^- , NH_4^+ , K^+ , Ca^{2+} , Mg^{2+} , Ti, Mn, Fe, Zn, Pb and As. An eight source-factor solution from the PMF analyses is selected for discussion because a factor number of eight are found to be optimum.

3. Results and discussion

3.1. Spatial-temporal variations of $\text{PM}_{2.5}$ mass concentrations

The annual and seasonal average $\text{PM}_{2.5}$ concentrations (mean \pm standard deviation, units: $\mu\text{g m}^{-3}$) for the six sites are presented in Table 2. The ensemble average $\text{PM}_{2.5}$ concentration is $142.6 \pm 102.6 \mu\text{g m}^{-3}$, with a range of average values from $76.7 \pm 42.4 \mu\text{g m}^{-3}$ at BRR in summer to $178.6 \pm 104.6 \mu\text{g m}^{-3}$ at MMF in winter. The latter is more than four times higher than the latest China $\text{PM}_{2.5}$ Class II air quality standard ($35 \mu\text{g m}^{-3}$, GB 3095-2012). The highest daily average $\text{PM}_{2.5}$ concentration ($512.6 \mu\text{g m}^{-3}$) is found at MGH on 17 January 2010 and the lowest ($23.6 \mu\text{g m}^{-3}$) at BRR on 17 July 2010—this amounts to a maximum 21-fold difference between the highest and lowest daily average. The $\text{PM}_{2.5}$ concentrations exceeded $50 \mu\text{g m}^{-3}$ on more than

71.9% of the sampling days at BRR, and exceeded $100 \mu\text{g m}^{-3}$ on more than 78.1% of the sampling days at MMF.

BRR is employed as a reference station: it is located on the edge of Qingling Mountains, and only sporadic and insignificant pollution sources lie within 30 km of the site. Although lower than other five sites, the annual $\text{PM}_{2.5}$ concentration of $76.7 \mu\text{g m}^{-3}$ at BRR is still high, over 2 times the latest $\text{PM}_{2.5}$ standard in China. According to daily air quality data from the Environmental Monitoring Station of Xi'an (EMS Xi'an, <http://www.xianemc.gov.cn>), the $\text{PM}_{2.5}$ concentrations at BRR are considerably higher when winds are from northeast wind compared with airflow from other directions. This indicates that BRR is significantly influenced by the outflow of pollutants from the city and its surroundings under the prevailing northeasterly winds (Figs. 1 and S2).

The arithmetic mean $\text{PM}_{2.5}$ loadings showed the following pattern: MMF ($178.6 \mu\text{g m}^{-3}$) > MGH ($172.6 \mu\text{g m}^{-3}$) > IEE ($166.4 \mu\text{g m}^{-3}$) > CBE ($151.3 \mu\text{g m}^{-3}$) > GLC ($103.7 \mu\text{g m}^{-3}$) > BRR ($76.7 \mu\text{g m}^{-3}$) (red solid line in Fig. 2). The difference between the highest and the lowest annual mean $\text{PM}_{2.5}$ concentrations for the four urban sampling sites is $27.3 \mu\text{g m}^{-3}$, this amounts to 17% of the annual mean $\text{PM}_{2.5}$ concentration for four urban sites. More important, this relatively small difference suggests some degree of uniformity in the $\text{PM}_{2.5}$ loadings at the urban sites. The $\text{PM}_{2.5}$ annual mean values at two rural and four urban sites

Table 1
Characteristics of the six sampling sites.

Site (abbreviation)	Longitude (E)	Latitude (N)	N ^a	Surrounding environment
Gaoling county (GLC)	109°05'12.11"	34°32'05.34"	56	Rural, upwind (northeast) of Xi'an, farmland and village
Chan-ba ecological district (CBE)	109°01'21.66"	34°20'18.54"	56	Urban (northeast) a modern, ecological agriculture zone
Municipal government hall (MGH)	108°56'58.49"	34°16'01.08"	56	In the old city wall, a downtown administrative and residential area
Micro motor factory (MMF)	108°53'55.22"	34°15'59.65"	56	Next to the old city wall to the west, roadside in a commerce zone
Institute of Earth Environment, Chinese Academy of Sciences (IEE)	108°52'58.72"	34°13'49.77"	56	Urban (southwest) roadside at high-tech industrial zone
Black River reservoir (BRR)	108°12'21.27"	34°02'51.05"	56	Reference, downwind (southwest), on the edge of the Qingling Mountains.

^a N = Number of samples collected.

Table 2
Annual average concentrations \pm standard deviations of PM_{2.5} mass and chemical species at six sampling sites during 2010 in Xi'an (units: $\mu\text{g m}^{-3}$, 24-h samples taken from 10:00 am to 10:00 am the following day for two weeks during January, April, July and October 2010).

	Site ^a						All sites
	GLC	BRR	CBE	MGH	MMF	IEE	
N ^b	56	56	56	56	56	56	336
PM _{2.5}	103.7 \pm 76.6	76.7 \pm 42.4	151.3 \pm 100.5	172.6 \pm 109.8	178.6 \pm 104.6	166.4 \pm 121.7	142.6 \pm 102.6
OC	15.3 \pm 17.8	7.7 \pm 5.7	18.8 \pm 17.4	20.3 \pm 19.8	23.8 \pm 22.7	24.2 \pm 24.0	18.6 \pm 19.6
EC	5.0 \pm 3.4	2.9 \pm 1.6	7.5 \pm 6.0	7.6 \pm 6.4	9.1 \pm 7.6	7.6 \pm 6.1	6.7 \pm 5.8
Cl ⁻	3.8 \pm 5.6	1.3 \pm 1.3	5.8 \pm 5.4	5.6 \pm 5.3	6.5 \pm 5.6	6.6 \pm 6.6	5.0 \pm 5.5
NO ₃ ⁻	18.6 \pm 19.5	9.3 \pm 8.1	20.7 \pm 18.3	21.5 \pm 17.2	18.5 \pm 13.7	18.5 \pm 15.1	17.8 \pm 15.9
SO ₄ ²⁻	21.2 \pm 16.5	13.5 \pm 8.9	25.5 \pm 19.1	27.6 \pm 19.1	25.8 \pm 14.9	24.3 \pm 16.3	23.1 \pm 16.6
NH ₄ ⁺	8.3 \pm 7.6	4.3 \pm 2.8	8.2 \pm 9.4	9.9 \pm 9.6	9.8 \pm 8.8	8.6 \pm 8.8	8.3 \pm 8.3
K ⁺	1.9 \pm 2.6	0.7 \pm 0.5	1.6 \pm 1.3	1.9 \pm 1.7	1.8 \pm 1.5	1.8 \pm 1.8	2.5 \pm 1.7
Ca ²⁺	1.3 \pm 2.3	1.4 \pm 1.4	4.6 \pm 5.1	4.3 \pm 2.8	5.3 \pm 5.2	4.7 \pm 7.6	3.6 \pm 4.8
Mg ²⁺	0.2 \pm 0.2	0.1 \pm 0.1	0.6 \pm 0.5	0.5 \pm 0.3	0.5 \pm 0.3	0.7 \pm 1.2	0.4 \pm 0.6
Ti	0.1 \pm 0.1	0.1 \pm 0.1	0.1 \pm 0.3	0.1 \pm 0.1	0.1 \pm 0.2	0.1 \pm 0.2	0.1 \pm 0.2
Mn	0.1 \pm 0.1	0.1 \pm 0.0	0.1 \pm 0.1				
Fe	0.9 \pm 1.5	1.2 \pm 1.5	1.6 \pm 3.3	1.5 \pm 1.3	1.8 \pm 2.4	1.5 \pm 2.1	1.4 \pm 2.1
Zn	0.6 \pm 0.4	0.2 \pm 0.1	1.9 \pm 1.8	1.6 \pm 1.3	1.9 \pm 1.8	2.2 \pm 2.7	1.4 \pm 1.8
Pb	0.2 \pm 0.2	0.1 \pm 0.1	0.3 \pm 0.3	0.3 \pm 0.3	0.3 \pm 0.3	0.3 \pm 0.4	0.3 \pm 0.3
As	0.0 \pm 0.0	0.0 \pm 0.0	0.0 \pm 0.0	0.0 \pm 0.0	0.0 \pm 0.0	0.0 \pm 0.0	0.0 \pm 0.0

^a Abbreviations for the sites as in Table 1.

^b N = number of samples.

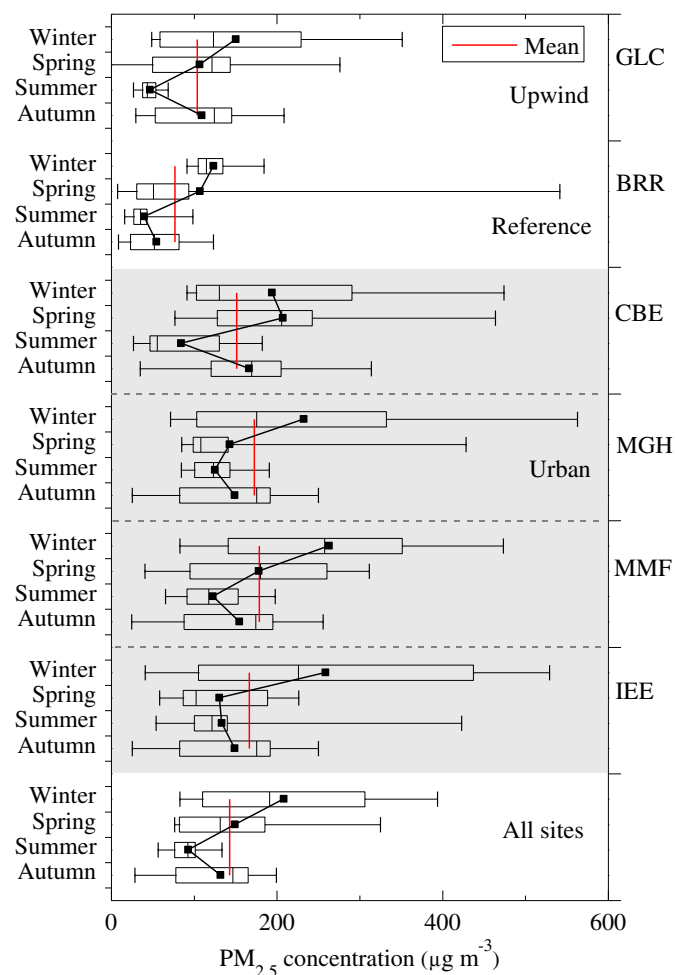


Fig. 2. Seasonal and annual PM_{2.5} concentrations at the six sites. Arithmetic seasonal mean (squares), median (vertical bars in boxes), 25th and 75th percentiles (lower and upper bars), minimum and maximum () concentrations, and annual mean (vertical red lines) for each chemical component for each site.

are 90.2 and 167.2 $\mu\text{g m}^{-3}$, respectively; the difference between urban and rural sampling sites is 77 $\mu\text{g m}^{-3}$ (60%, the average relative percent difference). The fact that the difference of urban–rural sites is not that large suggests that the PM_{2.5} loadings at the rural site are affected by outflow from Xi'an urban and surrounding areas. This highlights the fact that PM_{2.5} pollution continues to be a serious issue in Xi'an.

Along these lines, the coefficient of divergence (CD) of the annual mean concentrations of PM_{2.5} species between two different types of sampling sites can be used to assess the extent of pollutant diffusion in a given area (Wongphatarakul et al., 1998; Zhang and Friedlander, 2000). The CD, a self-normalized parameter, is calculated as follows:

$$CD_{jk} = \sqrt{\frac{1}{p} \sum_{i=1}^p \left(\frac{X_{ij} - X_{jk}}{X_{ij} + X_{jk}} \right)^2} \quad (1)$$

where x_{ij} represents the average concentration for a chemical component i at site j , and k represent the two sampling sites, and p is the number of chemical components. For our study, if the two sampling groups of sites are similar, the CD would approach zero, but if they are very different, the CD would approach unity (Wongphatarakul et al., 1998). Fig. S1 shows that the CD for the mean PM_{2.5} levels for the suite of analytes at four urban sites (IEE, MMF, MGH and CBE) and those in two rural sites (BRR and GLC) is 0.2, this low value indicates a moderate level of uniformity in the PM_{2.5} chemical composition over the spatial scale of the study (Xi'an has an area of 1066 km²).

The PM_{2.5} mass concentrations exhibited clear seasonal variations, with maxima in winter and minima in summer; the mean loadings for the six sites combined decreased in the order: winter (202.6 $\mu\text{g m}^{-3}$) > spring (145.8 $\mu\text{g m}^{-3}$) > autumn (140.9 $\mu\text{g m}^{-3}$) > summer (91.5 $\mu\text{g m}^{-3}$) (black solid line with the square box in Fig. 2). This is generally consistent with previous studies on PM_{2.5} mass loadings, which have shown high concentrations in winter and low ones in summer (Cao et al., 2012a; Han et al., 2009). While a winter maximum and summer minimum are found at all sites except CBE, there are differences in the spring and autumn ranks at the six sites. For one group, composed of GLC and MGH, the winter maxima and summer minima are clear, and the concentrations in autumn and spring are nearly the same. A second group (MMF and BRR) had the winter maxima and summer minima, but the springtime loadings at these two sites are higher than in autumn. IEE is the only station that showed a minimum in

spring, but the difference between the spring and summer means there is small.

CBE is the only station that showed a springtime maximum, and this can be explained by the influence of mineral dust on $PM_{2.5}$ loadings there. Xi'an is located on the margin of the vast Loess Plateau, and mineral dust from arid and semiarid areas to the north and northwest is frequently transported to Xi'an in spring (Zhang et al., 2002). This presumably caused higher $PM_{2.5}$ mean concentrations in spring compared with in autumn. The influence of the dust storms also is evident at BRR, and the chemical data supporting this argument are presented below.

The difference between the highest seasonally-averaged $PM_{2.5}$ mass concentration in winter ($202.6 \mu\text{g m}^{-3}$ at six sites on average) and lowest one in summer ($91.5 \mu\text{g m}^{-3}$) is $111.1 \mu\text{g m}^{-3}$. This amounts to 76% (the relative percent difference) of the annual mean $PM_{2.5}$ concentration for six sites, and it is slightly higher than the difference (60%) between two rural and four urban sites as mentioned above. This result indicates that the $PM_{2.5}$ seasonal variability is greater than the spatial variations among the six sites. It is noteworthy that the highest $PM_{2.5}$ concentration ($206.9 \mu\text{g m}^{-3}$ for spring at CBE) may have been related to the 2010 Xi'an International Horticultural Exposition because extensive construction activities for that event generated large quantities of fugitive dust.

3.2. Spatial and temporal variations of $PM_{2.5}$ chemical species

3.2.1. Carbonaceous species

Fig. 3 shows the spatial and temporal variations of the carbonaceous species at the six sites. The overall average mass concentrations of the OC and EC components in $PM_{2.5}$ are $18.6 \mu\text{g m}^{-3}$ and $6.7 \mu\text{g m}^{-3}$, respectively (Table 2). The maximum OC concentration is $116.1 \mu\text{g m}^{-3}$; this occurs at IEE on 17 January 2010, and the maximum EC ($32.2 \mu\text{g m}^{-3}$) is at MMF on the same day. The lowest concentrations of both OC ($2.5 \mu\text{g m}^{-3}$) and EC ($0.8 \mu\text{g m}^{-3}$) occur at BRR on 17 July 2010. The difference between the OC maximum and minimum is $113.6 \mu\text{g m}^{-3}$, which is more than 6 times the mean $PM_{2.5}$ OC concentration for the six sites. The difference in maximum to minimum EC concentrations is $31.4 \mu\text{g m}^{-3}$, and that is more than 4.5 times the grand average (Fig. 3(b) and Table 2). These results show that the variability in OC is greater than that of EC, and this is presumably due to the relatively stable emissions for EC and the fact that OC includes both primary

OC (POC), which is produced directly from combustion and other processes, and secondary OC (SOC) produced by gas-to-particle conversion. In addition, the Relative Standard Deviations (RSD) for EC and OC are 87% and 105%, which support this argument.

The amount of TC relative to the mean $PM_{2.5}$ mass decreases in the order IEE (19.7%) > MMF (17.4%) > CBE (17.3%) > GLC (16.4%) > MGH (15.4%) > BRR (14.8%) (red solid line in Fig. 3(a)). Two sites, IEE and MMF, are located near roads, and therefore motor vehicle emissions probably impact the carbonaceous fine particles at those sites. Seasonally, the patterns in $TC/PM_{2.5}$ are generally similar to those of the $PM_{2.5}$ loadings themselves, with winter maxima and summer minima; overall, the $TC/PM_{2.5}$ ratio decreased in the order winter > spring > autumn > summer (maroon solid line with circle in Fig. 3(a)).

The ratio of OC/EC has been used as an indicator of the sources for the carbonaceous aerosol. Prior studies have shown that the primary OC/EC ratios for coal combustion, motor vehicle emissions, and biomass burning are 2.7, 1.1, and 9.0, respectively (Cachier et al., 1989; Watson et al., 2001). A study of Chinese sources similarly showed that the OC/EC ratios from coal combustion and biomass burning are much higher than those from motor vehicle emissions (Cao et al., 2005b). In this study, the OC/EC ratios decrease in the order IEE (3.3) > BRR (2.9) > MMF (2.8) > MGH (2.8) > GLC (2.7) > CBE (2.6) (blue solid line in Fig. 3(a)). The overall average OC/EC ratio is 2.9, and because this value is close to the OC/EC ratio for coal combustion, that is the likely source for much of the carbonaceous aerosol. This argument also is supported by the high loadings of SO_4^{2-} and several trace elements.

The OC/EC ratios showed seasonal variability, with the ratios decreasing from winter to spring to autumn to summer (black solid line with square in Fig. 3(a)); this pattern is similar to the seasonality in $PM_{2.5}$ mass loadings. The wintertime maximum can be explained by the extensive burning of coal for domestic heating; the emissions from this source would increase the OC loadings relative to EC in $PM_{2.5}$ (blue bar in Fig. 3(b)).

3.2.2. Water-soluble inorganic ions

The major water-soluble inorganic ions are sulfate, nitrate and ammonium ($\sum \text{SNA}$) (Wang et al., 2005) and the arithmetic mean SO_4^{2-} , NO_3^- and NH_4^+ concentrations are $23.1 \mu\text{g m}^{-3}$, $17.8 \mu\text{g m}^{-3}$ and $8.3 \mu\text{g m}^{-3}$, respectively (Table 2). Fig. 4 shows the spatial and temporal variations of $\sum \text{SNA}/PM_{2.5}$ ratios at the six sites. The mean $\sum \text{SNA}/PM_{2.5}$ ratios decreased in the order GLC (42.1%) > BRR (38.3%) > MGH (35%) > CBE

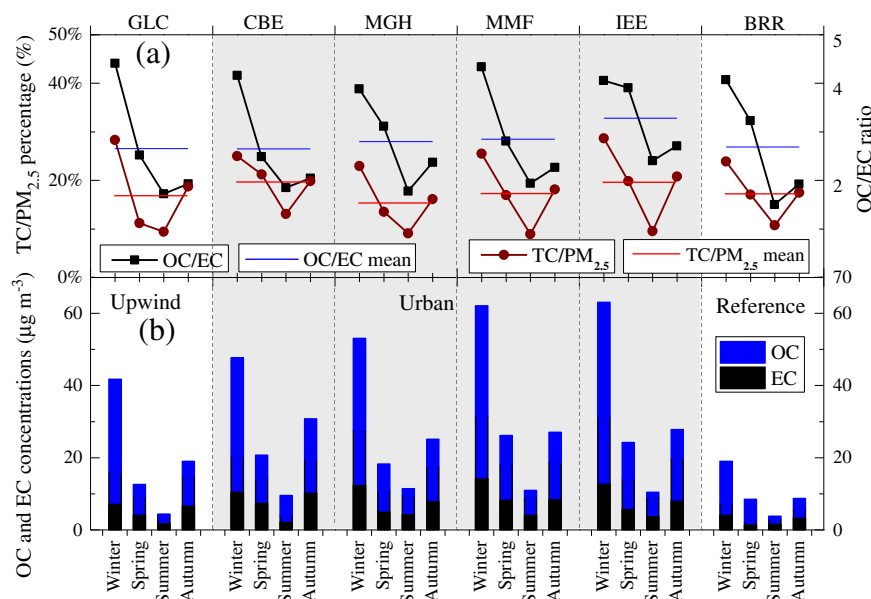


Fig. 3. Seasonal average organic carbon and elemental carbon (OC and EC) concentrations, OC/EC ratios, and $TC (= OC + EC)/PM_{2.5}$ ratios for the six study sites.

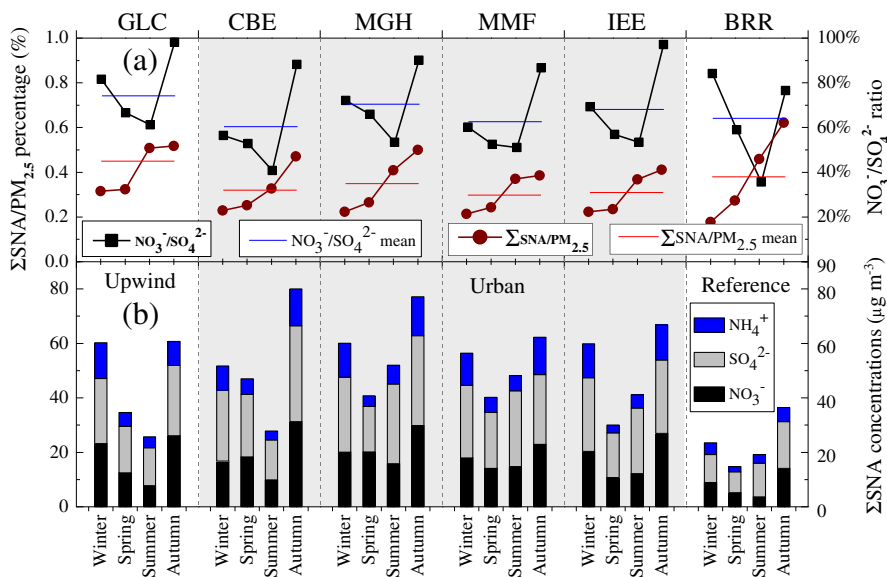


Fig. 4. Seasonality in water soluble ions Σ SNA ($= \text{SO}_4^{2-} + \text{NO}_3^- + \text{NH}_4^+$), $\text{NO}_3^-/\text{SO}_4^{2-}$ ratios and Σ SNA/ $\text{PM}_{2.5}$ mass percentages for each of the study sites.

(32%) > IEE (31%) > MMF (29.8%) (red solid line in Fig. 4(a)). It is clear that the Σ SNA/ $\text{PM}_{2.5}$ values at the two rural sites are higher than those at four city sites, and this is due to the lower $\text{PM}_{2.5}$ concentrations in the suburbs.

With reference to seasonality, the trends in Σ SNA/ $\text{PM}_{2.5}$ ratios are not consistent with those exhibited by the $\text{PM}_{2.5}$ mass concentrations or the $\text{TC}/\text{PM}_{2.5}$ ratios. That is, the Σ SNA/ $\text{PM}_{2.5}$ ratios followed an increasing trend from winter < spring < summer < autumn (maroon solid line with circle in Fig. 4(a)). Elevated levels of nitrate and sulfate occurred in summer and autumn (Fig. 4(b)), and this is consistent with the temporal variability in the mechanisms that lead to their formation. Indeed, the high temperatures and conditions favorable for photo-oxidation and gas-phase transformations can explain the higher concentrations of the secondary inorganic species in the warmer months. Stable conditions near the surface at that time of year also would limit the diffusion of pollutants.

The $\text{NO}_3^-/\text{SO}_4^{2-}$ mass ratio has been used as an indicator of the relative importance of stationary versus mobile sources for atmospheric

sulfur and nitrogen (Arimoto et al., 1996; Yao et al., 2002). Spatially, the $\text{NO}_3^-/\text{SO}_4^{2-}$ average values follow the order GLC (0.77) > MGH (0.7) > IEE (0.65) > BRR (0.64) > MMF (0.63) > CBE (0.6) (blue solid line in Fig. 4(a)). The average $\text{NO}_3^-/\text{SO}_4^{2-}$ ratio (0.65) at the two rural sites (GLC and BRR) is similar to that for the urban sites (0.64). Seasonally, the $\text{NO}_3^-/\text{SO}_4^{2-}$ ratios increased from summer to spring to winter to autumn (black solid line with squares in Fig. 4(a)), and this pattern held at all six sites. Elevated $\text{NO}_3^-/\text{SO}_4^{2-}$ ratios in autumn indicate that a greater proportion of the $\text{PM}_{2.5}$ originated from motor vehicle exhaust compared with other times of the year.

The seasonal patterns of other ions are shown in Fig. 5. Soluble K^+ most often is enriched in the aerosol as a result of biomass burning (Andreae, 1983; Watson et al., 2001), and it can be seen in Fig. 5(c) with royal square that the mean K^+ concentrations are much higher winter ($6.1 \mu\text{g m}^{-3}$) compared with the other seasons (autumn = 1.4, spring = 1.2, and summer = $0.8 \mu\text{g m}^{-3}$). This is more than likely due to the burning of wheat straw and maize stalks for heat in the rural areas around Xi'an. Cl^- (the dark yellow square in

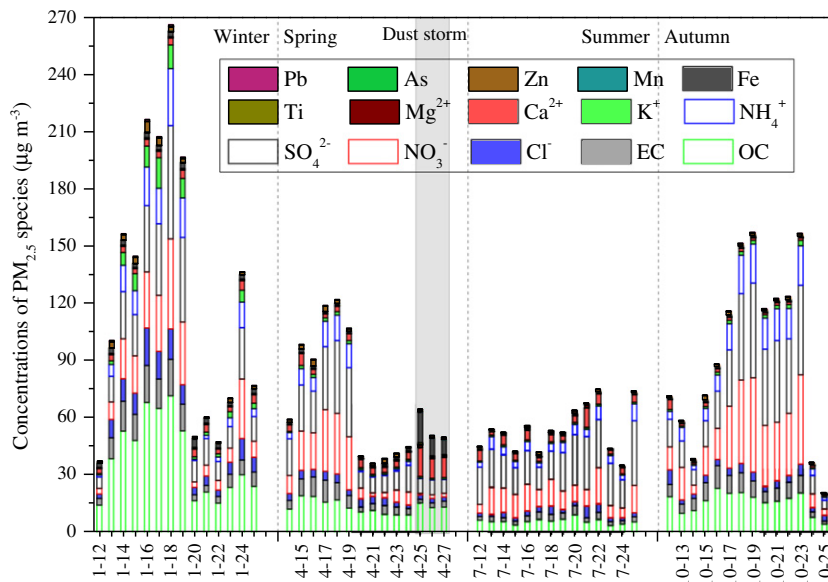


Fig. 5. Daily average variations of $\text{PM}_{2.5}$ species for the six sites combined in Xi'an during 2010.

Fig. 5(c)) shows the same seasonal pattern as K^+ , that is, winter ($9.5 \mu\text{g m}^{-3}$) > autumn ($3.9 \mu\text{g m}^{-3}$) > spring ($3.4 \mu\text{g m}^{-3}$) > summer summer ($2.7 \mu\text{g m}^{-3}$).

Water-soluble Ca^{2+} concentrations in $\text{PM}_{2.5}$ have been used as an indicator of mineral dust, and Asian dust typically exhibits its highest concentrations in late winter and early spring (Cao et al., 2005a; Shen et al., 2007). Prior studies in Xi'an have shown that soil dust from long-range transport together with fugitive dust, that is, dust from roads, construction activities, and traditional street sweeping, cause high dust loadings in spring in Xi'an, and this leads to high Ca^{2+} concentrations (Shen et al., 2008; Zhang et al., 2002). In our study, the Ca^{2+} loadings (in $\mu\text{g m}^{-3}$) in $\text{PM}_{2.5}$ show the following order: spring (5.4) > summer > winter (3.5) > autumn (1.7) (the yellow square in Fig. 5(c)). Mg^{2+} concentrations ($\mu\text{g m}^{-3}$) show the same seasonal patterns as Ca^{2+} , that is spring (0.7) > summer (0.6) > winter (0.5) > autumn (0.2) (the magenta square in Fig. 5(c)). During a strong dust event (25–27 April 2010, LT cyan ribbon in Fig. 5) that occurred during our study, the mean Ca^{2+} and Mg^{2+} concentrations are 12 and $1.1 \mu\text{g m}^{-3}$, respectively. Another peak in Ca^{2+} and Mg^{2+} are found in summer, and these are most likely caused by construction dusts (Fig. 5(c)) due to high calcium concentration ($5.63 \mu\text{g m}^{-3}$, arithmetic mean) has been reported on the Loess Plateau by Wen (Wen, 1989).

3.2.3. Inorganic elements

The overall mean concentrations of six trace elements (Ti, Mn, Fe, Zn, Pb and As) in the $\text{PM}_{2.5}$ samples are 0.1, 0.1, 1.4, 1.4, 0.3 and $0.02 \mu\text{g m}^{-3}$, respectively (Table 2). Ti, Fe and Mn are most often considered crustal elements because their main source is mineral dust, and they are often used to markers for this material. Zn is generally enriched in the aerosol as a result of emissions from smelters and metallurgical industries (Dall'Osto et al., 2013). Pb gasoline additives are phased out in China in 2000 (Xu et al., 2012), but Pb, As, and various other elements are enriched in Chinese coal, and these elements are typically show concentrations in the atmosphere significantly above natural levels (Tian et al., 2011; Wang et al., 2006).

Indeed, the As/Fe and Pb/Fe ratios have been used as indicators of fly ash from uncontrolled coal combustion (Cao et al., 2012a). The As/Fe and Pb/Fe ratios in our study are 0.03 ± 0.03 and 0.28 ± 0.25 , respectively. These values are much higher than those in Toronto, ON, Canada (0.007 and 0.062) (Lee et al., 2003), Mexico City, Mexico (0.006 and 0.068) (Vega et al., 2004) or Seattle, WA, USA (0.015 and 0.099) (Maykut et al., 2003), but they are similar to those for 14 Chinese cities (winter and summer) (0.04 ± 0.03 and 0.39 ± 0.32 , respectively) (Cao et al., 2012a). The strong Pb/As correlation ($R = 0.71$, $n = 269$, $p < 0.005$) is further evidence that coal ash is a more important source for Pb than the residues from leaded gasoline, and this is consistent with the conclusions from studies of Pb isotopic ratios in Xi'an (Xu et al., 2012).

It can be seen from Fig. 5(d and e) that peaks in the concentrations of the crustal elements (Fe, Ti and Mn) occurred in winter but more notably during a strong dust storm in spring; Ca^{2+} and Mg^{2+} did not show the wintertime peak, but these two ions did show the dust storm spike and another one in summer (Fig. 5(c)). Two peaks are seen in the concentrations of the trace elements Zn, Pb and As, one in winter and the other in autumn, and these are linked to seasonal pollution episodes, including haze/fog events (Cao et al., 2012b). Seasonal covariations in the patterns of crustal elements and trace elements imply a significant level of consistency in their respective sources.

3.2.4. $\text{PM}_{2.5}$ mass closure

Fig. 6 presents the seasonal and spatial variations in $\text{PM}_{2.5}$ mass closure as calculated from the concentrations of organic matter, EC, inorganic ions, soil dust, and unidentified material. Organic matter (OM) is estimated as $1.6 \times \text{OC}$ (Chen and Yu, 2007; El-Zanan et al., 2009), and this is done to account for the unmeasured hydrogen and oxygen atoms. Soil dust is estimated as $25 \times \text{Fe}$ (Cao et al., 2008; Wu et al.,

2011) to account for the unmeasured oxygen and other elements. Overall (left-hand panel in Fig. 6), the contributions in order of importance are OM (19.3%) > soil dust (16.8%) > sulfate (15.5%) > other ions (11.4%) > nitrate (11.1%) > ammonium (5.4%) > elemental carbon (4.5%) at all study sites combined.

Spatially (middle panel of Fig. 6), the main components of $\text{PM}_{2.5}$ are in roughly similar proportions at each of the four urban sites (17–21.3% for OM, 14.1–16.6% for SO_4^{2-} and 9.5–11.1% for NO_3^-). In comparison, the percentages of these components at GLC are 22.8% for OM, 19.6% for SO_4^{2-} and 17% for NO_3^- and thus higher than those at the four urban sites. This suggests that pollutants at the upwind GLC site are transported over regional scales, and they presumably can affect Xi'an under the prevailing northeasterly flow. Industrial sulfur dioxide emission intensities (mass of SO_2 emissions per unit GDP) in Weinan ($34^\circ 30' \text{N}$, $109^\circ 38' \text{E}$), a city ~60 km upwind of Xi'an, have been used to infer the regional transport of pollutants. The SO_2 emission intensities in 2010 are 2.51 and $35.91 \text{ kg per ten thousand yuan}$ at Xi'an and Weinan, respectively (Yearbook, 2011). This shows a potential pool of pollutants upwind of the study sites. In addition, recent research has shown that industrial sources in Xi'an – for example, the Xi'an Aircraft Industry Group and coal-related sources (Xi'an North Heating Ltd.) in the upwind Yanliang District (Fig. 1) – can influence Xi'an's air quality (Zhang and Gu, 2013).

The $\text{PM}_{2.5}$ at the BRR reference site is mainly composed of soil dust (33.9%) and OM (13.7%). High concentrations of calcium carbonate have been found over the Loess Plateau; for instance, an arithmetic mean of calcium concentration ($5.63 \mu\text{g m}^{-3}$) has been reported by Wen (1989) for Weinan sampling site, which is on the Loess Plateau. Calcium from fugitive dust also has been shown to be high at BRR, with TSP, PM_{10} , $\text{PM}_{2.5}$ and PM_1 levels of 6.0, 8.3, 6.8 and $7.7 \mu\text{g m}^{-3}$, respectively (Cao et al., 2008). In addition, the extensive forests on the Qinling Mountains cover 48% of the land surface, and these heavily vegetated areas emit large quantities of VOCs, which can be oxidized to form a particulate OC (<http://www.snly.gov.cn/>). These well-established sources for dust and OC are the most reasonable explanations for the main components of $\text{PM}_{2.5}$ observed at BRR.

Distinctive seasonality is evident for most of the aerosol species (right-hand panel in Fig. 6); this is manifest as increased proportions of $\text{PM}_{2.5}$ as follows: OC in winter, soil dust in spring, sulfate in summer and nitrate in autumn. In winter, increased emissions from heating sources together with low temperatures and shallow planetary boundary layer heights evidently led to higher pollutant concentrations. This is particularly evident in the enhanced OC loadings, which can be explained by a combination of primary OC emissions and secondary OC formation. Previous studies showed that 44% of the TC could be attributed to coal burning during the winter of 2003 (Cao et al., 2005b), and coal combustion is the main source for primary OC (Cao et al., 2011a; Zhang et al., 2007). In spring, frequent dust intrusions cause significant impacts on air quality, and this is seen in elevated concentrations of soil components, including Ca^{2+} , Mg^{2+} . In summer, sulfate concentrations would be expected to increase with the higher temperatures because the oxidation rates for SO_2 would be relatively rapid, but on the other hand, the concentrations of semi-volatile components (such as nitrate and organics) on particles should have decreased because their concentrations the gas phase relative to the particulate phase would be increased by the higher temperatures. In autumn, heterogeneous reactions favor the formation nitrate, and the stable weather conditions that frequently occur in north China limit the dispersal of pollutants: these two factors can explain the high nitrate concentrations that we observed.

3.3. $\text{PM}_{2.5}$ source apportionment

The average composition of the eight factors generated by the PMF analysis based on annual data is shown in Figs. S3 (the four urban sites) to S4 (the two rural sites). The data inputs to PMF models for the four urban and two rural sites are the arithmetic mean values and

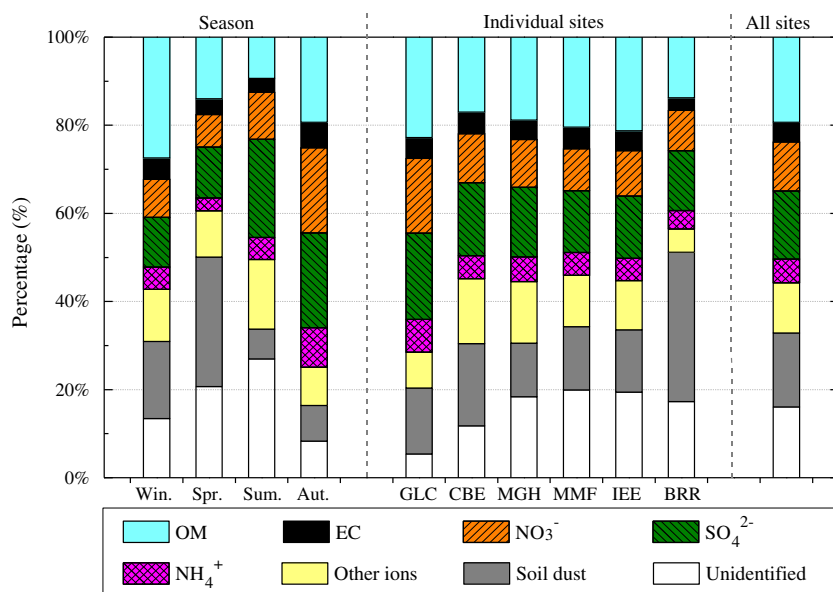


Fig. 6. Spatial and temporal variations of $PM_{2.5}$ species mass closure by study site. Organic matter (OM) is estimated as $1.6 \times OC$ (Chen and Yu, 2007; El-Zanan et al., 2009) to account for unmeasured hydrogen and oxygen. Soil dust is estimated as $25 \times Fe$ (Cao et al., 2008; Wu et al., 2011) to account for unmeasured oxygen and non-iron minerals. "Unidentified" is the mass that remains after subtracting the sums of the individual from the measured $PM_{2.5}$ mass.

standard deviations. Eight potential sources produced by the model are coal combustion, vehicle emissions, secondary inorganic sulfate, secondary inorganic nitrate, geological materials, construction dust, biomass burning and industrial emissions.

The first component, coal combustion, is loaded with SO_4^{2-} , and it also had high loadings of OC and EC. As and Pb, which as previously mentioned have high concentrations in Chinese coal (Tian et al., 2011; Wang et al., 2006), also are associated with this source. Coal is the primary energy source for many industries in China, and it is extensively burnt for domestic heating, and coal burring is concluded to be the main source for primary OC and EC in prior studies (Cao et al., 2011a; Zhang et al., 2007). The second source, motor vehicle emissions, is loaded with NO_3^- and EC, two species known to be enriched in vehicular emissions (Dall'Osto et al., 2013; Tian et al., 2011). The third source is secondary inorganic sulfate, which are typically characterized by SO_4^{2-} . The fourth source is secondary inorganic nitrate, which are typically characterized by NO_3^- . The fifth source, geological material, is typically characterized by high concentrations of crustal elements, including Ti, Fe and Mn. The sixth source is construction dust (including fugitive dust and resuspended road dust), and Ca^{2+} and Mg^{2+} have been used as indicators for this material in Xi'an (Shen et al., 2010). Although the construction dust also contains crustal elements, such as Ti and Fe, it is prevalent in the urban cities of China, and no effective measures for construction dust control are implemented, as well as sampling sites are located at the Loess Plateau. Therefore, calcium is used as a main indicator element for construction dust in Xi'an (Cao et al., 2008; Shen et al., 2010). The seventh identified as emissions from biomass burning, is characterized by high K^+ , which has been used extensively as tracer of biomass-burning aerosols (Cachier and Ducret, 1991; Chow et al., 1994; Duan et al., 2004). High Cl^- has been ascribed to marine or sea salt aerosol source in some studies (Lee et al., 1999), but in the interior of China, it is more likely to be from coal/biomass burning (Yao et al., 2002) (white bars in Figs. S3 and S4). The Eighth source is assigned to industrial pollution because of the high Zn content; this element is known to be enriched in aerosols as a result of emissions from smelters and a variety of metallurgical industries (Dall'Osto et al., 2013).

Fig. 7 shows the relative contributions from each identified source to the $PM_{2.5}$ loadings broken down by annual average concentrations for both the rural and urban sites. The contributions of the sources generated by the PMF analyses are calculated by multiple regression of the G

matrix (Paatero, 1997) against the measured mass concentrations. Of the eight source categories for $PM_{2.5}$ at the four urban sites (Fig. 7(a)), secondary inorganic aerosol (including secondary inorganic sulfate and secondary inorganic nitrate) is found to be the most important contributor to fine particles, accounting for 29.6% of total $PM_{2.5}$ mass on average. This is followed by coal combustion (18.5%), vehicle emissions (14.9%), industrial emissions (10.8%), geological material (10.0%), biomass-burning emissions (9.0%) and construction dust (7.3%). In comparison, for the two rural sites (Fig. 7(b)), the order of the sources from largest to smallest is secondary inorganic aerosol (31.7%), coal combustion (15.9%), biomass burning (13.3%), vehicle emissions (12.9%), crustal soil (11.8%), construction dust (7.5%) and industrial emissions (7%).

In short, the main contribution of the secondary inorganic aerosol to the $PM_{2.5}$ mass at the rural sites (31.7%) is slightly higher compared with the urban sites (29.6%). If the contributions from the four main sources (secondary inorganic aerosol, coal combustion, vehicle emission and biomass burning) in urban/rural were combined, fossil fuel burning-related emissions might dominate $PM_{2.5}$ pollution in Xi'an, representing ~74.1% (four urban sampling sites) and ~73.8% (two rural sampling sites) of $PM_{2.5}$. These results of the PMF analysis are consistent with the daily average variations of $PM_{2.5}$ loading and its species (Fig. 5) and with the mass closure assessments presented above (Fig. 6), further supporting the notion that $PM_{2.5}$ in Xi'an is mainly from anthropogenic sources, especially combustion sources. These source profiles for the four urban sampling sites are consistent with the results of several earlier studies. For instance, PMF analysis indicated that secondary aerosols and coal combustion are the major sources (30 and 21%, respectively) for PM_1 during 2008 (Shen et al., 2010) and combustion emissions (52.2%, the sum of coal combustion and secondary aerosols) for $PM_{2.5}$ during 2009 (Cao et al., 2012b) in Xi'an.

3.4. Comparisons of $PM_{2.5}$ at different sites

Fig. 8 presents the percentages of the major chemical species (OC, EC, SO_4^{2-} , NO_3^- , NH_4^+) that made up the bulk of $PM_{2.5}$ in our study along with the mass ratios of OC/EC and NO_3^-/SO_4^{2-} (partial data) in fine particles. These data are presented with the results from previous studies in Xi'an (Cao et al., 2005b, 2007, 2011b, 2012a; Han et al., 2010; Shen et al., 2011; Zhang et al., 2011; Zhu et al., 2010)

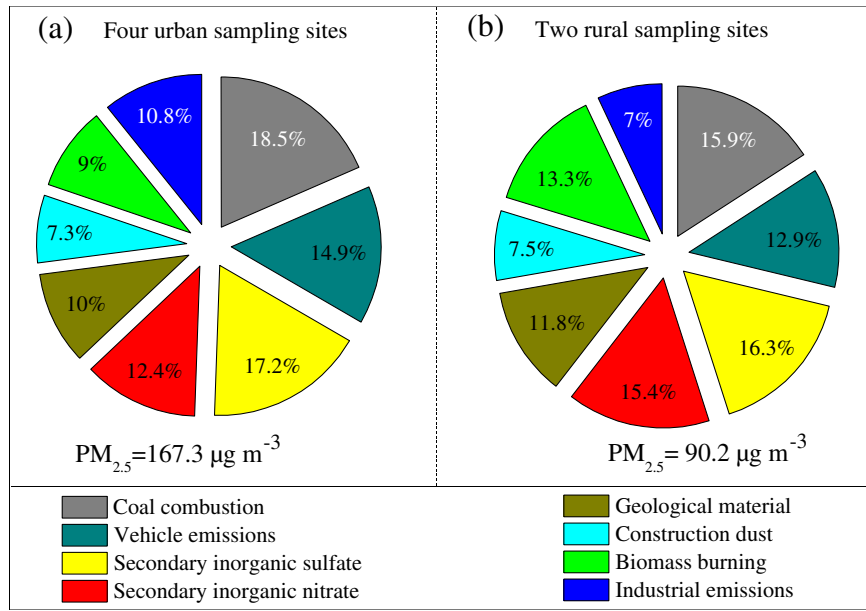


Fig. 7. Positive matrix factorization (PMF) resolved source contributions to PM_{2.5} (annual average concentrations) at four urban sites (a) and two rural sites (b).

(Fig. 8(a)), representative megacities in China (Ho et al., 2002; Yang et al., 2011b; Ye et al., 2003) and other major cities (Heo et al., 2009; Y.P. Kim et al., 2000; Lonati et al., 2008; Vega et al., 2004) (Fig. 8(b)) (see Tables S1 and S2 for detailed information). Unlike several megacities in China (Table S1), the main component of PM_{2.5} from Xi'an is SO₄²⁻, and this reflects the importance of coal combustion emissions. OC is the most important contributor to the fine particle mass at Beijing, Shanghai, Guangzhou and Chongqing, and SO₄²⁻ the second most abundant species at those sites.

The OC/EC ratios at Xi'an, Shanghai and Hong Kong are 2.8, 2.6 and 1.6, respectively (black square in Fig. 8(b)), and these differences can

be explained by the main sources for the carbonaceous particles. Shanghai is home to a large harbor, and therefore diesel emissions from ships are likely a major contributor to EC there (Ye et al., 2003). Meanwhile, the dominant source for EC at the Hong Kong sampling site, which is at Hong Kong Polytechnic University, is thought to be motor vehicle emissions (Ho et al., 2002). Again, the high OC/EC ratios at Xi'an are an indication that the PM_{2.5} carbonaceous species in are mainly from coal combustion emissions. From 2003 to 2010, a decreasing trend in the OC/PM_{2.5} ratio (blue bar in Fig. 8(a)) is observed, and this is due to a decrease in the OC/EC ratio (black square in Fig. 8(a)) because the EC/PM_{2.5} ratio (gray bar in Fig. 8(a)) remained relatively

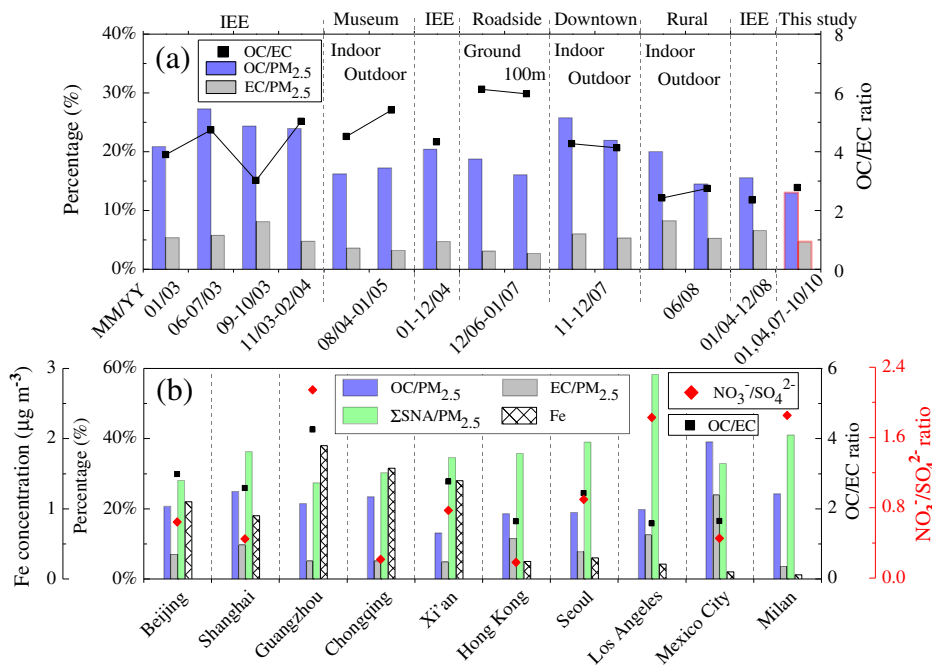


Fig. 8. Comparison of percentages of the major chemical species contributing to PM_{2.5} from this study with (a) previous measurements in Xi'an and (b) representative megacities across China and other major cities worldwide. References for the previous studies in Xi'an are Cao et al. (2005b, 2007, 2011b, 2012a), Han et al. (2010), Shen et al. (2011), Zhang et al. (2011), and Zhu et al. (2010). References for the regional comparisons are Beijing (Yang et al., 2011b), Shanghai (Ye et al., 2003), Guangzhou (Yang et al., 2011b), Chongqing (Yang et al., 2011b), Hong Kong (Ho et al., 2002), Seoul (Heo et al., 2009), Los Angeles (B.M. Kim et al., 2000), Mexico City (Vega et al., 2004) and Milan (Lonati et al., 2008).

constant. This pattern suggests that the municipal government's long-term efforts to curb polluting emissions achieved some level of success during the 11th Five-Year-Plan (FYP) (2005–2010).

The ratios of $\text{NO}_3^-/\text{SO}_4^{2-}$ in Xi'an, Chongqing, Guangzhou and Shanghai are 0.8, 0.2, 2.1 and 0.5, respectively (red diamond in Fig. 8(b)), and this indicates that motor vehicle exhaust is an important source for some water-soluble inorganic ions in Xi'an. Comparisons of our results with those from megacities outside of China show that soil dust (bar with grid in Fig. 8(b)) – as represented by Fe as a marker element – is a more important contributor to $\text{PM}_{2.5}$ in Xi'an relative to the other cities. Representative dust concentrations in $\mu\text{g m}^{-3}$ are as follows: Xi'an (1.4), Mexico City (0.1), Seoul (0.3), Los Angeles (0.2) and Milan (0.06) (see Table S2 for detailed information).

4. Conclusions

The daily $\text{PM}_{2.5}$ concentrations in Xi'an during 2010 showed an average of $142.61 \pm 102.65 \mu\text{g m}^{-3}$; this is over four times the national ambient air quality standard (GB3095-2012) in China. Spatial variability is not very evident, but seasonal patterns are observed. The increases in $\text{PM}_{2.5}$ are mainly due to OC in winter; soil dust in spring; and sulfate and nitrate in summer and autumn, respectively. Seasonal variations of $\text{TC}/\text{PM}_{2.5}$ and OC/EC ratios are similar to the trends in $\text{PM}_{2.5}$ mass concentrations. In contrast, the seasonality in the $\sum \text{SNA}/\text{PM}_{2.5}$ ratios showed a different pattern, with high values in autumn and low ones in winter. The $\text{NO}_3^-/\text{SO}_4^{2-}$ ratios also are different, with high values in autumn and low values in summer.

Eight presumptive sources for $\text{PM}_{2.5}$ are uncovered by the PMF analysis; these are coal combustion, motor vehicles, secondary inorganic sulfate, secondary inorganic nitrate, geological material, construction dust, biomass burning and industrial activities. The source apportionment results further supported the notion that emissions from fossil fuel burning are the main cause of $\text{PM}_{2.5}$ pollution in Xi'an. A decreasing trend in the $\text{OC}/\text{PM}_{2.5}$ ratios is seen in comparisons with previous studies from 2003 to 2010 in Xi'an; this suggests that pollution control efforts of the local government have had some positive effects.

Conflict of interest statement

We declare that we have no financial and personal relationships with other people or organizations that can inappropriately influence our work; there is no professional or other personal interest of any nature or kind in any product, service and/or company that could be construed as influencing the position presented in, or the review of, the manuscript entitled, Spatial and seasonal variations of $\text{PM}_{2.5}$ mass and chemical species during 2010 in Xi'an, China.

Acknowledgments

This study was supported by the National Natural Science Foundation of China (41230641), and projects from "Strategic Priority Research Program" of the Chinese Academy of Science (XDB05060500), Ministry of Science & Technology (201209007), and Shaanxi Government (2012KTZB03-01-01).

Appendix A. Supplementary data

Supplementary data to this article can be found online at <http://dx.doi.org/10.1016/j.scitotenv.2014.11.007>.

References

Andreae MO. Soot carbon and excess fine potassium: long-range transport of combustion-derived aerosols. *Science* 1983;220:1148–51.
 Antony Chen LW, Watson JG, Chow JC, Magliano KL. Quantifying $\text{PM}_{2.5}$ source contributions for the San Joaquin Valley with multivariate receptor models. *Environ Sci Technol* 2007;41:2818–26.

Antony Chen LW, Watson JG, Chow JC, DuBois DW, Herschberger L. Chemical mass balance source apportionment for combined $\text{PM}_{2.5}$ measurements from U.S. non-urban and urban long-term networks. *Atmos Environ* 2010;44:4908–18.
 Arimoto R, Duce RA, Savoie DL, Prospero JM, Talbot R, Cullen JD, et al. Relationships among aerosol constituents from Asia and the North Pacific during PEM-West A. *J Geophys Res Atmos* 1996;101:2011–23.
 Cachier H, Ducret J. Influence of biomass burning on equatorial African rains. *Nature* 1991;352:228–30.
 Cachier H, Bremond MP, Buatmenard P. Carbonaceous aerosols from different tropical biomass burning sources. *Nature* 1989;340:371–3.
 Cao JJ, Lee SC, Ho KF, Zhang XY, Zou SC, Fung K, et al. Characteristics of carbonaceous aerosol in Pearl River Delta Region, China during 2001 winter period. *Atmos Environ* 2003;37:1451–60.
 Cao JJ, Lee SC, Ho KF, Zou SC, Fung K, Li Y, et al. Spatial and seasonal variations of atmospheric organic carbon and elemental carbon in Pearl River Delta Region, China. *Atmos Environ* 2004;38:4447–56.
 Cao JJ, Lee SC, Zhang XY, Chow JC, An ZS, Ho KF, et al. Characterization of airborne carbonate over a site near Asian dust source regions during spring 2002 and its climatic and environmental significance. *J Geophys Res Atmos* 2005a;110:D03203.
 Cao JJ, Wu F, Chow JC, Lee SC, Li Y, Chen SW, et al. Characterization and source apportionment of atmospheric organic and elemental carbon during fall and winter of 2003 in Xi'an, China. *Atmos Chem Phys* 2005b;5:3127–37.
 Cao JJ, Lee SC, Chow JC, Watson JG, Ho KF, Zhang RJ, et al. Spatial and seasonal distributions of carbonaceous aerosols over China. *J Geophys Res Atmos* 2007;112:D22511.
 Cao JJ, Chow JC, Watson JG, Wu F, Han YM, Jin ZD, et al. Size-differentiated source profiles for fugitive dust in the Chinese Loess Plateau. *Atmos Environ* 2008;42:2261–75.
 Cao JJ, Shen ZX, Chow JC, Qi GW, Watson JG. Seasonal variations and sources of mass and chemical composition for PM_{10} aerosol in Hangzhou, China. *Particuology* 2009;7:161–8.
 Cao JJ, Chow JC, Tao J, Lee SC, Watson JG, Ho KF, et al. Stable carbon isotopes in aerosols from Chinese cities: influence of fossil fuels. *Atmos Environ* 2011a;45:1359–63.
 Cao JJ, Li H, Chow JC, Watson JG, Lee S, Rong B, et al. Chemical composition of indoor and outdoor atmospheric particles at Emperor Qin's Terra-cotta Museum, Xi'an, China. *Aerosol Air Qual Res* 2011b;11:70–9.
 Cao JJ, Shen ZX, Chow JC, Watson JG, Lee SC, Tie XX, et al. Winter and summer $\text{PM}_{2.5}$ chemical compositions in fourteen Chinese cities. *J Air Waste Manage Assoc* 2012a;62:1214–26.
 Cao JJ, Wang QY, Chow JC, Watson JG, Tie XX, Shen ZX, et al. Impacts of aerosol compositions on visibility impairment in Xi'an, China. *Atmos Environ* 2012b;59:559–66.
 Cao JJ, Zhu CS, Tie XX, Geng FH, Xu HM, Ho SSH, et al. Characteristics and sources of carbonaceous aerosols from Shanghai, China. *Atmos Chem Phys* 2013;13:803–17.
 Chan CK, Yao X. Air pollution in mega cities in China. *Atmos Environ* 2008;42:1–42.
 Chen X, Yu JZ. Measurement of organic mass to organic carbon ratio in ambient aerosol samples using a gravimetric technique in combination with chemical analysis. *Atmos Environ* 2007;41:8857–64.
 Chow JC, Watson JG, Fujita EM, Lu Z, Lawson DR, Ashbaugh LL. Temporal and spatial variations of $\text{PM}_{2.5}$ and PM_{10} aerosol in the Southern California air quality study. *Atmos Environ* 1994;28:2061–80.
 Dall'Osto M, Querol X, Alastuey A, O'Dowd C, Harrison RM, Wenger J, et al. On the spatial distribution and evolution of ultrafine particles in Barcelona. *Atmos Chem Phys* 2013;13:741–59.
 Dong F, He D, Zhao PS, Yang YD, Zhao XJ, Zhang WZ, et al. Characteristics of carbonaceous aerosol in the region of Beijing, Tianjin, and Hebei, China. *Atmos Environ* 2013;71:389–98.
 Duan FK, Liu XD, Yu T, Cachier H. Identification and estimate of biomass burning contribution to the urban aerosol organic carbon concentrations in Beijing. *Atmos Environ* 2004;38:1275–82.
 Duan FK, He KB, Ma YL, Yang FM, Yu XC, Cadle SH, et al. Concentration and chemical characteristics of $\text{PM}_{2.5}$ in Beijing, China: 2001–2002. *Sci Total Environ* 2006;355:264–75.
 Duan JC, Tan JH, Cheng DX, Bi XH, Sheng GY, et al. Sources and characteristics of carbonaceous aerosol in two largest cities in Pearl River Delta Region, China. *Atmos Environ* 2007;41:2895–903.
 El-Zanan HS, Zielinska B, Mazzoleni LR, Hansen DA. Analytical determination of the aerosol organic mass-to-organic carbon ratio. *J Air Waste Manage Assoc* 2009;59:58–69.
 Han YM, Cao JJ, Chow JC, Watson JG, An ZS, Liu SX. Elemental carbon in urban soils and road dusts in Xi'an, China and its implication for air pollution. *Atmos Environ* 2009;43:2464–70.
 Han YM, Cao JJ, Lee SC, Ho KF, An ZS, Engineering S, et al. Different characteristics of char and soot in the atmosphere and their ratio as an indicator for source identification in Xi'an, China. *Atmos Chem Phys* 2010;10:595–607.
 Han YM, Du PX, Cao JJ, Posmentier ES. Multivariate analysis of heavy metal contamination in urban dusts of Xi'an, China. *Science of the Total Environment* 2006;355:176–86.
 He KB, Yang FM, Ma YL, Zhang Q, Yao XH, Chan CK, et al. The characteristics of $\text{PM}_{2.5}$ in Beijing, China. *Atmos Environ* 2001;35:4959–70.
 Heo JB, Hopke PK, Yi SM. Source apportionment of $\text{PM}_{2.5}$ in Seoul, Korea. *Atmos Chem Phys* 2009;9:4957–71.
 Ho KF, Lee SC, Yu JC, Zou SC, Fung K. Carbonaceous characteristics of atmospheric particulate matter in Hong Kong. *Sci Total Environ* 2002;300:59–67.
 Ho KF, Lee SC, Chan CK, Yu JC, Chow JC, Yao XH. Characterization of chemical species in $\text{PM}_{2.5}$ and PM_{10} aerosols in Hong Kong. *Atmos Environ* 2003;37:31–9.
 Ho KF, Ho SSH, Lee SC, Kawamura K, Zou SC, Cao JJ, et al. Summer and winter variations of dicarboxylic acids, fatty acids and benzoic acid in $\text{PM}_{2.5}$ in Pearl Delta River Region, China. *Atmos Chem Phys* 2011;11:2197–208.
 Hopke PK. Recent developments in receptor modeling. *J Chemom* 2003;17:255–65.

- Hu M, Wu Z, Slanina J, Lin P, Liu S, Zeng L. Acidic gases, ammonia and water-soluble ions in PM_{2.5} at a coastal site in the Pearl River Delta, China. *Atmos Environ* 2008;42:6310–20.
- Huang K, Zhuang G, Li J, Wang Q, Sun Y, Lin Y, et al. Mixing of Asian dust with pollution aerosol and the transformation of aerosol components during the dust storm over China in spring 2007. *J Geophys Res Atmos* 2010;115:D00K13.
- Huang W, Cao JJ, Tao YB, Dai LZ, Lu SE, Hou B, et al. Seasonal variation of chemical species associated with short-term mortality effects of PM_{2.5} in Xi'an, a central city in China. *Am J Epidemiol* 2012;175:556–66.
- Hwang I, Hopke PK. Estimation of source apportionment and potential source locations of PM_{2.5} at a west coastal IMPROVE site. *Atmos Environ* 2007;41:506–18.
- Kawamura K, Wang GH, Cheng CL, Li JJ, Cao JJ, Zhang RJ, et al. Molecular distribution and stable carbon isotopic composition of dicarboxylic acids, ketocarboxylic acids, and α -dicarbonyls in size-resolved atmospheric particles from Xi'an City, China. *Environ Sci Technol* 2012;46:4783–91.
- Kim BM, Tefferi S, Zeldin MD. Characterization of PM_{2.5} and PM₁₀ in the South Coast Air Basin of Southern California: Part 1—spatial variations. *J Air Waste Manage Assoc* 2000a;50:2034–44.
- Kim YP, Moon KC, Lee JH. Organic and elemental carbon in fine particles at Kosan, Korea. *Atmos Environ* 2000b;34:3309–17.
- Lee E, Chan CK, Paatero P. Application of positive matrix factorization in source apportionment of particulate pollutants in Hong Kong. *Atmos Environ* 1999;33:3201–12.
- Lee PKH, Brook JR, Dabek-Zlotorzynska E, Mabury SA. Identification of the major sources contributing to PM_{2.5} observed in Toronto. *Environ Sci Technol* 2003;37:4831–40.
- Li W, Zhou S, Wang X, Xu Z, Yuan C, Yu Y, et al. Integrated evaluation of aerosols from regional brown hazes over northern China in winter: concentrations, sources, transformation, and mixing states. *J Geophys Res Atmos* 2011;116:D09301.
- Liu S, Hu M, Slanina S, He LY, Niu YW, Bruegemann E, et al. Size distribution and source analysis of ionic compositions of aerosols in polluted periods at Xinken in Pearl River Delta (PRD) of China. *Atmos Environ* 2008;42:6284–95.
- Lonati G, Giugliano M, Ozgen S. Primary and secondary components of PM_{2.5} in Milan (Italy). *Environ Int* 2008;34:665–70.
- Maykut NN, Lewtas J, Kim E, Larson TV. Source apportionment of PM_{2.5} at an urban IMPROVE site in Seattle, Washington. *Environ Sci Technol* 2003;37:5135–42.
- Paatero P. Least squares formulation of robust non-negative factor analysis. *Chemom Intell Lab Syst* 1997;37:23–35.
- Paatero P, Tapper U. Positive matrix factorization: a non-negative factor model with optimal utilization of error estimates of data values. *Environmetrics* 1994;5:111–26.
- Shen ZX, Cao JJ, Arimoto R, Zhang RJ, Jie DM, Liu SX, et al. Chemical composition and source characterization of spring aerosol over Horqin sand land in northeastern China. *J Geophys Res Atmos* 2007;112:D14315.
- Shen ZX, Arimoto R, Cao JJ, Zhang RJ, Li X, Du N, et al. Seasonal variations and evidence for the effectiveness of pollution controls on water-soluble inorganic species in total suspended particulates and fine particulate matter from Xi'an, China. *J Air Waste Manage Assoc* 2008;58:1560–70.
- Shen ZX, Cao J, Arimoto R, Han YM, Zhu CS, Tian J, et al. Chemical characteristics of fine particles (PM₁) from Xi'an, China. *Aerosol Sci Technol* 2010;44:461–72.
- Shen ZX, Cao JJ, Liu SX, Zhu CS, Wang X, Zhang T, et al. Chemical composition of PM₁₀ and PM_{2.5} collected at ground level and 100 meters during a strong winter-time pollution episode in Xi'an, China. *J Air Waste Manage Assoc* 2011;61:1150–9.
- Sun JM, Liu TS, Lei ZF. Sources of heavy dust fall in Beijing, China on April 16, 1998. *Geophys Res Lett* 2000;27:2105–8.
- Sun YL, Zhuang GS, Tang A, Wang Y, An Z. Chemical characteristics of PM_{2.5} and PM₁₀ in haze-fog episodes in Beijing. *Environ Sci Technol* 2006;40:3148–55.
- Tian HZ, Wang Y, Xue ZG, Qu YP, Chai FH, Hao JM. Atmospheric emissions estimation of Hg, As, and Se from coal-fired power plants in China, 2007. *Sci Total Environ* 2011;409:3078–81.
- Tie X, Geng F, Guenther A, Cao J, Greenberg J, Zhang R, et al. Megacity impacts on regional ozone formation: observations and WRF-Chem modeling for the MIRAGE-Shanghai field campaign. *Atmos Chem Phys* 2013;13:5655–69.
- Van Donkelaar A, Martin RV, Brauer M, Kahn R, Levy R, Verduzco C, et al. Global estimates of ambient fine particulate matter concentrations from satellite-based aerosol optical depth: development and application. *Environ Health Perspect* 2010;118.
- Vega E, Reyes E, Ruiz H, Garcia J, Sanchez G, Martinez-Villa G, et al. Analysis of PM_{2.5} and PM₁₀ in the atmosphere of Mexico City during 2000–2002. *J Air Waste Manage Assoc* 2004;54:786–98.
- Wang Y, Zhuang GS, Sun YL, An ZS. Water-soluble part of the aerosol in the dust storm season—evidence of the mixing between mineral and pollution aerosols. *Atmos Environ* 2005;39:7020–9.
- Wang MS, Zheng BS, Wang BB, Shehong LAH, Wu DS, Hu J. Arsenic concentrations in Chinese coals. *Sci Total Environ* 2006;357:96–102.
- Watson JG, Chow JC, Houck JE. PM_{2.5} chemical source profiles for vehicle exhaust, vegetative burning, geological material, and coal burning in Northwestern Colorado during 1995. *Chemosphere* 2001;43:1141–51.
- Wen QZ. Chinese loess geochemistry (in Chinese). Beijing: Science Press; 1989. p. 115–58.
- Wong CSC, Li XD, Zhang G, Qi SH, Peng XZ. Atmospheric deposition of heavy metals in the Pearl River Delta, China. *Atmos Environ* 2003;37:767–76.
- Wongphatarakul V, Friedlander SK, Pinto JP. A comparative study of PM_{2.5} ambient aerosol chemical databases. *Environ Sci Technol* 1998;32:3926–34.
- Wu F, Chow JC, Watson JG, An ZS, Cao JJ. Size-differentiated chemical characteristics of Asian paleo dust: records from aeolian deposition on Chinese Loess Plateau. *J Air Waste Manage Assoc* 2011;61:180–9.
- Xu HM, Cao JJ, Ho KF, Ding H, Han YM, Wang GH, et al. Lead concentrations in fine particulate matter after the phasing out of leaded gasoline in Xi'an, China. *Atmos Environ* 2012;46:217–24.
- Yang F, Huang L, Duan F, Zhang W, He K, Ma Y, et al. Carbonaceous species in PM_{2.5} at a pair of rural/urban sites in Beijing, 2005–2008. *Atmos Chem Phys* 2011a;11:7893–903.
- Yang F, Tan J, Zhao Q, Du Z, He K, Ma Y, et al. Characteristics of PM_{2.5} speciation in representative megacities and across China. *Atmos Chem Phys* 2011b;11:5207–19.
- Yao XH, Chan CK, Fang M, Cadle S, Chan T, Mulawa P, et al. The water-soluble ionic composition of PM_{2.5} in Shanghai and Beijing, China. *Atmos Environ* 2002;36:4223–34.
- Ye BM, Ji XL, Yang HZ, Yao XH, Chan CK, Cadle SH, et al. Concentration and chemical composition of PM_{2.5} in Shanghai for a 1-year period. *Atmos Environ* 2003;37:499–510.
- Yearbook SS. http://www.chinayearbook.com/yearbook/book_49070.htm, 2011.
- Zhang Z, Friedlander SK. A comparative study of chemical databases for fine particle Chinese aerosols. *Environ Sci Technol* 2000;34:4687–94.
- Zhang YW, Gu ZL. Air quality by urban design. *Nat Geosci* 2013;6:506–506.
- Zhang XY, Cao JJ, Li LM, Arimoto R, Cheng Y, Huebert B, et al. Characterization of atmospheric aerosol over Xi'an in the South Margin of the Loess Plateau, China. *Atmos Environ* 2002;36:4189–99.
- Zhang D, Iwasaka Y, Shi G, Zang J, Hu M, Li C. Separated status of the natural dust plume and polluted air masses in an Asian dust storm event at coastal areas of China. *J Geophys Res Atmos* 2005;110:D06302.
- Zhang RJ, Cao JJ, Lee SC, Shen ZX, Ho KF. Carbonaceous aerosols in PM₁₀ and pollution gases in winter in Beijing. *J Environ Sci (China)* 2007;19:564–71.
- Zhang T, Cao JJ, Tie XX, Shen ZX, Liu SX, Ding H, et al. Water-soluble ions in atmospheric aerosols measured in Xi'an, China: seasonal variations and sources. *Atmos Res* 2011;102:110–9.
- Zhang RJ, Jing J, Tao J, Hsu SC, Wang GH, Cao JJ, et al. Chemical characterization and source apportionment of PM_{2.5} in Beijing: seasonal perspective. *Atmos Chem Phys* 2013;13:7053–74.
- Zheng M, Salamon LG, Schauer JJ, Zeng L, Kiang CS, Zhang Y, et al. Seasonal trends in PM_{2.5} source contributions in Beijing, China. *Atmos Environ* 2005;39:3967–76.
- Zhu CS, Cao JJ, Tsai CJ, Shen ZX, Ho KF, Liu SX. The indoor and outdoor carbonaceous pollution during winter and summer in rural areas of Shaanxi, China. *Aerosol Air Qual Res* 2010;10:550–8.